

Asymmetric control mechanisms of bimanual coordination:
an application of directed connectivity analysis to
kinematic and functional MRI data

Yohko Maki

DOCTOR OF
PHILOSOPHY

Department of Physiological Sciences
School of Life Science
The graduate University for Advanced Studies

2008

CONTENTS

1. Abstract.....	3
2. Introduction.....	4
3. Materials and Methods.....	10
4. Results.....	19
5. Discussion	22
6. Conclusion.....	30
7. Acknowledgement.....	31
8. Reference.....	32
9. Table.....	43
10. Figures.....	45
11. Appendix.....	49

ABSTRACT

Mirror-symmetrical bimanual movement is more stable than parallel bimanual movement. This is well established at the kinematic level. I used functional MRI (fMRI) to evaluate the neural substrates of the stability of mirror-symmetrical bimanual movement. Right-handed participants ($n = 17$) rotated disks with their index fingers bimanually, both in mirror-symmetrical and asymmetrical parallel modes. I applied the Akaike causality model to both kinematic and fMRI time-series data. I hypothesized that kinematic stability is represented by the extent of neural “cross-talk”: as the fraction of signals that are common to controlling both hands increases, the stability also increases. The standard deviation of the phase difference for the mirror mode was significantly smaller than that for the parallel mode, confirming that the former was more stable. I used the noise-contribution ratio (NCR), which was computed using a multivariate autoregressive model with latent variables, as a direct measure of the cross-talk between both the two hands and the bilateral primary motor cortices (M1s). The mode-by-direction interaction of the NCR was significant in both the kinematic and fMRI data. Furthermore, in both sets of data, the NCR from the right hand to the left was more prominent than vice versa during the mirror-symmetrical mode, whereas no difference was observed during parallel movement or rest. The asymmetric interhemispheric interaction from the left M1 to the right M1 during symmetric bimanual movement might represent cortical-level cross-talk, which contributes to the stability of symmetric bimanual movements.

INTRODUCTION

Bimanual coordination in the mirror-symmetrical mode, in which homologous muscles are active simultaneously, is more stable than in the parallel mode, in which homologous muscles are engaged in an alternating fashion (Swinnen et al., 1997). When a subject performs a cyclical movement in the parallel mode, increasing the movement frequency ultimately results in a phase transition towards the mirror-symmetrical mode, but the opposite transition does not occur (Kelso, 1984). This phenomenon was first formalized theoretically by dynamic-systems theory at the behavioral level (Haken et al., 1985; Schöner and Kelso, 1988). Furthermore, the reversal in direction at the phase transition was mainly associated with the non-dominant hand (Walter and Swinnen, 1992; Byblow et al., 1994, 1998, 2000; Sherwood, 1994; Semjen et al., 1995; Treffner and Turvey, 1995; Rogers et al., 1998; Garry and Franks, 2000). These kinematic data suggest that the left hemisphere is dominant for bimanual movement.

To associate the process of bimanual coordination with the neural structures that control hand movements (de Oliveira, 2002), the concepts of inter-manual and neural cross-talk (Marteniuk and MacKenzie, 1980) have been introduced. Interactions between the movements of the two hands (inter-manual cross-talk) are assumed to result from neural cross-talk at multiple levels between the signals controlling the two limbs. The lowest level of cross-talk supposedly occurs downstream from the specification of movement parameters, possibly through the ipsilateral corticospinal tract (Cattaert et al., 1999), as each effector receives signals from both contralateral and ipsilateral descending pathways. The mirror-symmetrical

condition requires the activation of homologous muscles, and so the signals of both pathways are always congruent. By contrast, the parallel condition requires non-homologous muscles to be activated, and so conflict between crossed and uncrossed cortical pathways might arise (cross-talk). This is supported by the findings of Kagerer et al. (2003), who reported that participants in whom transcranial magnetic stimulation (TMS) elicited distal ipsilateral motor-evoked potentials exhibited higher variability during a bimanual parallel circling task than participants whose ipsilateral pathways could not be activated transcranially. This suggests that the common signal sent to both effectors through the contralateral and ipsilateral pathways enhanced the stability of mirror-symmetrical movement as compared to parallel movement, resulting in the increased variability during parallel movement (Cattaert et al., 1999).

Cross-talk might also occur at a higher level through interhemispheric interaction (Kennerley et al., 2002). Kennerley et al. (2002) reported that callosotomy patients exhibited a lack of temporal coupling during continuous circle drawing, with the two hands oscillating at non-identical frequencies. They concluded that synchronization between the hands depends on interhemispheric transmission across the corpus callosum.

Several neuroimaging studies support the concept that interhemispheric interaction exists during the phase transition. Meyer-Lindenberg et al. (2002) demonstrated neuronal dynamics conforming to the predictions made by the non-linear system theory. Using positron-emission tomography (PET), they depicted the cortical regions related to the extent of behavioral instability, assuming that

neuronal activity in these “unstable” areas increases as the frequency of the movement increases. Within these areas, they found that minor disruption by double-pulse TMS to the right dorsal premotor cortex (PMd) evoked large-scale phase transitions in participants’ performance. Meyer-Lindenberg et al. (2002) concluded that an increase in behavioral instability corresponds to increasing neural instability represented in the right PMd.

Using event-related functional MRI (fMRI), Aramaki et al. (2006a) depicted the transition-related activity in multiple right-lateralized parieto-premotor regions. These areas were different from the regions activated by bimanual movement execution. Aramaki et al. (2006a) concluded that at the phase transition, the cortical neural cross-talk occurs in distributed networks upstream of the primary motor cortex through asymmetric interhemispheric interaction.

These studies imply that there is some “default” setting by which the two hands are linked together to produce identical motor output, and that an additional mechanism is required to uncouple the hands in order to generate different movements (Evans and Baker, 2003). However, the neural substrates of the default linking that makes bimanual mirror-symmetrical movement so stable have remained unknown, particularly at the cortical level.

The purpose of the present study was to delineate the cortical cross-talk that stabilizes mirror-symmetrical movement. Using fMRI, I compared the kinematic relationship between both hands and the neural relationship between the primary motor cortices of both hemispheres during mirror-symmetrical and parallel bimanual cyclical movements. I focused on cross-talk at the level of the bilateral primary motor cortices

(M1s), where movement parameters are specified and transmitted to the effectors.

I used a continuous circle-drawing task instead of a discrete movement task, such as tapping, for mainly technical reasons: continuous kinematic data are more easily handled by the multivariate autoregressive (MAR) model of time-series analysis. Previously, it was supposed that the neural substrates for continuous bimanual coordination might differ from those for discrete movements (Kennerley et al., 2002; Spencer et al., 2003). In split-brain patients, bimanual coordination during discrete tasks was well preserved (Preilowski, 1972; Franz et al., 1996; Ivry and Hazeltine, 1999), whereas coordination was impaired during a continuous bimanual task (Kennerley et al., 2002). However, this does not necessarily restrict the transcallosal neural cross-talk to the continuous cyclical movements (Bonzano, et al., 2008).

Previous kinematic studies (Stucchi and Viviani, 1993; Semjen et al., 1995; Treffner and Turvey, 1995, 1996; Swinnen et al., 1996; Byblow et al., 2000; Kennerley et al., 2002) have indicated right hand dominance. Previous clinical and imaging studies have shown that the left hemisphere is dominant for the representation of motor skills (Sirigu et al., 1996; Haaland et al., 2000), including bimanual coordination (Serrien et al., 2003). Accordingly, I predicted that asymmetric cross-talk from the left M1 to the right M1 is more prominent than vice versa.

I further hypothesized that this asymmetric cortical cross-talk is more prominent during mirror-symmetrical movement than during asymmetric parallel movement. During the mirror-symmetrical mode, the movement command from the dominant left hemisphere would facilitate, or at least not negatively influence,

symmetric movements. In this sense, the cross-talk at the cortical level during mirror movement can be understood as a gating of the signal from one hemisphere to its homonymous counterpart, in order to ensure shared neural control of the movements of both limbs in which homologous muscles are to be activated. During the asymmetric parallel mode, by contrast, there would be ongoing interference due to conflicting information. Parallel asymmetric movement usually requires a greater workload than mirror-symmetrical movement, which is represented as more prominent activation in the supplementary motor area (SMA) and the right PMd (Sadato et al., 1997). Double-pulse TMS of the right PMd caused a phase shift from the parallel mode to the mirror mode (Meyer-Lindenberg et al., 2002). Thus, this additional workload was interpreted as the conversion of the motor program or the suppression of conflicting information issued in the left hemisphere to its right counterpart, and hence no gating occurred during the parallel mode.

As signal gating might not be depicted by the increment of the neural activity, I adopted statistical time-series modeling. The MAR model represents a general statistical time-series model that propagates information from the past to the future. The Akaike noise-contribution ratio (NCR; Akaike, 1968) quantifies the portion of the power-spectral density of an observed variable from the independent noise of the MAR, which becomes a measure of causality among variables. It allows interpretation of the causality from one hand to the other, or from the motor cortex of one hemisphere to the other. Thus, the extent of cross-talk can be quantified by the causality that is represented by the NCR. Unlike the mathematical formulation of the dynamic-systems model that is usually employed to deal with the relative phase via a

differential equation in order to evaluate the stability of the system (Haken et al., 1985; Schöner and Kelso, 1988; Meyer-Lindenberg et al., 2002; Kennerley et al., 2002), which cannot be directly applied to neuroimaging datasets, the MAR can be applied to both kinematic data and neural activities. According to our *a-priori* hypothesis, the gating might be represented as the asymmetric NCR from the left M1 to the right M1, which, in turn, brings the asymmetric NCR from the right hand to the left hand during mirror-symmetrical movement more prominently than during parallel movement.

MATERIALS AND METHODS

Participants

In total, 19 subjects participated in the fMRI study. None of the subjects had a history of psychiatric or neurological illness. The protocol was approved by the Ethical Committee of the National Institute of Physiological Sciences, Japan. All subjects gave their written informed consent for participation in the study. During the experiment, I stopped the testing of one subject due to stomach pain, and one subject fell asleep; the data from these two subjects were excluded from the analysis. The 17 participants included in the analysis comprised eight men and nine women, aged between 20 and 32 years, all of whom were strongly right-handed according to the Edinburgh Handedness Inventory (mean score \pm standard deviation [SD] = 0.956 ± 0.072 ; Oldfield, 1971).

Subject setup

The subjects lay supine in a 3.0 Tesla MR scanner (Allegra; Siemens, Erlangen, Germany). Their elbows and wrists were slightly flexed and relaxed so that each hand could be placed on the non-ferromagnetic frames set over the participant's body. On the frame, two discs were placed on both sides of the subject (Figure 1). Each disc was attached to the MRI-compatible rotary encoder (HEDS5701, Hewlett-Packard, Palo Alto, CA; spatial resolution = 1°) to register finger movements at a sampling rate of 1,000 Hz. The encoders were connected to a personal computer (Dimension 8200; Dell Computer, Round Rock, TX) to record the rotation-related time-series data. As the axial length of the magnet was 130 cm, both hands were outside of the magnet. In this position, the subjects could not see their

finger movements. To minimize head motion, I used tight but comfortable foam padding placed around each subject's head. For visual and auditory stimulus presentation, I used Presentation 0.92 (Neurobehavioral Systems, Albany, CA) software implemented on a personal computer (Dimension 8200; Dell Computer, Round Rock, TX). A liquid-crystal display projector (DLA-M200L; Victor, Yokohama, Japan) located outside and behind the scanner projected instruction cues and a cross-hair onto a translucent screen. Subjects viewed the screen via a mirror attached to the head coil of the MRI scanner. The subjects wore MRI-compatible headphones (Hitachi, Yokohama, Japan). I did not measure electromyographic activity during the fMRI, mainly because of movement-related artifacts due to the movement of electrical leads caused by bimanual coordination.

Tasks

The subjects performed an auditory-paced bimanual disk-rotation task. They were asked to rotate the discs with their index fingers. To ensure constant timing and an equal number of cycles across conditions, the bimanual movements were paced by auditory cues at 0.6 Hz. The auditory cues (260 Hz, 50 ms) were administered continuously through the headphones during the scanning session (both task and rest periods). The volume of the sound was adjusted for each subject to an appropriate level for task execution, taking into account the MR scanner noise. Subjects performed both mirror-symmetrical and parallel movements. In the mirror-symmetrical mode, the directions of rotation were symmetrical with regard to the midline of the body in the outward direction (the right hand moved the disk in a clockwise direction whereas the left hand moved the disk in a counterclockwise

direction). During the parallel mode, both hands rotated in the same clockwise direction. A task session consisted of a 180-sec task period with rest periods before (15 sec) and after (20 sec) the task period. Each subject performed nine sessions: three sessions in the parallel mode, three sessions in the mirror-symmetrical mode, and three rest sessions. The baseline periods were added for the functional definition of the M1s by contrasting them with the 180-sec task condition. As I aimed to evaluate the causality during the parallel mode and the mirror mode, I obtained the longer-term data separately for each condition.

MRI data acquisition

A time-course series of 215 volumes was acquired in each session using T2*-weighted gradient echo-planar imaging (EPI) sequences. To maximize the sampling time points within an appropriate session duration that did not cause fatigue among the subjects (< 4 min), the interval between two successive acquisitions of the same image (the repetition time [TR]) was set to 1,000 ms. Each volume consisted of 17 axial slices (the maximum number of slices at a TR of 1,000 ms). The slice thickness was 3 mm with a 0.45-mm gap. The slices covered a region extending from the top of the head to the anterior commissure–posterior commissure line (AC–PC line), including both M1s for all of the subjects. The echo time (TE) was 30 ms. The flip angle (FA) was 65°. The transaxial field of view (FOV) was 192 mm, and the in-plane matrix size was 64 × 64 pixels with a pixel dimension of 3 × 3 × 3 mm. The images were scanned in a descending manner.

For anatomical imaging, T1-weighted magnetization-prepared rapid-acquisition gradient-echo (MP-RAGE) images were obtained (TR = 2,500 ms;

TE = 4.38 ms; FA = 8°; FOV = 230 mm (one slab); distant factor = 50%; number of slices per slab = 192; voxel dimensions = 0.9 × 0.9 × 1.0 mm) to cover the entire cerebral and cerebellar cortices.

Time-series analysis of kinematic data

1. Preprocessing of time-series data

Time-series data were extracted for 170 sec following the initiation of the task. As the spatial resolution of the encoder was 1°, a time resolution higher than 10 Hz would not give useful information, so the data were down-sampled to a sampling rate of 10 Hz. The linear trend of the increase or decrease of the data was subtracted using first-order differences; as the recording device accumulated the rotated angles, the data included monotonic increases or decreases in a gradient of roughly 216°/sec, which was caused by the rotation rate of 0.6 Hz (movement in an anticlockwise direction was recorded as increasing, and movement in a clockwise direction was recorded as decreasing). In this way, the preprocessed data indicated any deviation from the expected movement (°/sec).

2. Stability

The phase difference between hands was computed by subtracting the phase angle of both hands every 100 ms. During the mirror-symmetrical mode, both hands moved in opposite directions, and so the absolute values of the phase angle were used to calculate the phase difference. To obtain the signed relative phase, the phase of the left hand was subtracted from that of the right hand, and so negative values indicated a phase delay of the right hand. The signed phase difference at the

initiation of the movement, the average, and the SD throughout the session were calculated. The SD of the phase difference was used as an estimate of the stability of the mode of movement (Swinnen et al., 1996).

3. Modeling and quantifying directional connectivity

The causal relationship between the index fingers in the different movement modes (parallel, mirror-symmetrical, and rest) were studied. A statistical time-series model was fitted to the data in order to explain the spatiotemporal dynamics of the data and the causal relationships between the movements of both hands. An AR model can be used to elucidate the propagation of information from the past to the future; however, it is difficult to describe causal relationships when the driving noise variances are highly correlated (Yamashita et al., 2005; Wong and Ozaki, 2007). One solution is to obtain data at a finer temporal resolution; another is to include a hidden variable to absorb the common dynamic among the variables (Wong and Ozaki, 2007). Besides the two oscillations that explained the individual dynamics of each hand, I introduced a hidden variable to measure the dynamics that were common to both the left hand and the right hand. The two time-series were reconstructed to these three oscillations, which were mutually orthogonal. The following state-space model was applied:

$$\text{State equation} \quad x_t = Fx_{t-1} + G\omega_t$$

$$\text{Observation equation} \quad y_t = Hx_t + \varepsilon_t$$

Here, y_t denotes the preprocessed data. These data were projected from the state vector x_t through a projection matrix H . x_t was assumed to follow from first-order multivariate AR dynamics through the transition matrix F , and was driven

by multivariate Gaussian noise $G\omega_t$. x_t usually has a higher dimension than y_t . ε_t represents the bivariate Gaussian noise. In this paper, F , G , and H were designed in a particular parameterization structure, which is included in Appendix A.

Directional causality was quantified using the NCR, which is the proportion of spectral power corresponding to the causal variable (Akaike, 1968). The NCR gives a proportion of directional causality over the frequency interval from 0 Hz to the Nyquist frequency, which was 5 Hz in this study. The calculation of the NCR is straightforward (Wong and Ozaki, 2007). The spectral power over the frequency band of each component was computed using Simpson's numerical integration rule. The contribution of the three components was obtained by normalizing the corresponding integrated spectral power. Hereafter, I refer to the NCR in this integrated form.

For example, the left-hand oscillation can be explained by the linear summation of the contribution of the left-hand component, the contribution of the right-hand component, and that of the common component, all of which are normalized so that the sum of the three components is 1. In the same way, the right-hand oscillation can be explained by the linear summation of the NCR of the left-hand component, the NCR of the right-hand component, and that of the common component.

The NCR values of different subjects were collected and included in the two-way analysis of variance (ANOVA), which incorporated the effects of the direction of contribution (right hand to left hand vs. vice versa) and the mode (parallel vs. mirror-symmetrical).

fMRI data

1. Preprocessing

The first five volumes of each fMRI session were discarded because of unsteady magnetization. The data were analyzed using statistical parametric mapping (SPM5; Wellcome Department of Imaging Neuroscience, London, UK; Friston et al., 1995a; Friston et al., 1995b; Friston et al., 2007) implemented in Matlab (Mathworks, Sherborn, MA). Following slice-timing correction, the fMRI data were realigned to the first image for head-motion correction. The realigned data were then coregistered to the anatomical MRI. Finally, the fMRI data were spatially smoothed using a Gaussian kernel of 4 mm full width at half maximum in the x , y , and z axes. Anatomical normalization was not performed to avoid possible artifacts.

2. Region of interest (ROI) definition

The ROI of the M1s was defined on an anatomical and functional basis without spatial normalization. This was intended to avoid any artifacts accompanying the spatial normalization processes. For the first step, the ROIs were identified by means of the data from the task sessions analyzed with SPM software. A general linear model was used to identify voxels with task-related signal changes (Friston et al., 1995b). The signal time-course of each subject was modeled with two boxcar functions (that is, parallel and mirror-symmetrical movement), convolved with a hemodynamic-response function, high-pass filtering (128 sec), and session effects. To test hypotheses about regionally-specific condition effects, the estimates for each condition were compared by means of the linear contrasts. The resulting set of voxel values for each comparison constituted a statistical parametric map of the

t-statistic ($SPM\{t\}$). The threshold for the $SPM\{t\}$ was set at a highly conservative family-wise error rate (FWE) of $p < 0.001$. M1 was defined by the activation peaks that were located on the hand-knob segment of the precentral gyrus by visual inspection; the hand knob is a reliable landmark for identifying the hand motor area (Yousry et al., 1997; Figure 2). When the activation peaks were not found on the hand knob, the activation peaks closest to the hand knob were selected. In fact, a lack of hand representation at the hand knob was observed in three subjects (two unilateral left and one unilateral right). However, all of them showed hand representation at the bilateral central sulci adjacent to the hand knob. Table 1 shows the individually defined M1s in which the coordinates were normalized into space registered by the Montreal Neurological Institute (MNI) coordinates, in order to confirm that the ROI definition was appropriate.

3. Time-series data extraction

The non-smoothed time-series data of each coordinate were extracted using MarsBaR software (<http://marsbar.sourceforge.net/>) in a spherical ROI (radius = 3 mm). The time-series data of the two ROIs were extracted from nine sessions for each subject (three each of the parallel, mirror-symmetrical, and rest sessions). The 10 points (10 sec) from the beginning of the movement were discarded to exclude the influence of any instability due to movement initiation.

4. Modeling and quantifying directional connectivity

The state-space modeling was applied to the preprocessed fMRI time-series data. The idea of a hidden variable was applied again with a modification of the

parameterization (for a detailed explanation, see Appendix B). For each set of time-series data, the AR order p was chosen using the Akaike Information Criterion (AIC), such that the model with the smallest AIC was selected. Similar to kinematic data, the NCR was calculated from the estimated state-space models. The NCR values for different subjects were collected to use in the two-way ANOVA incorporating the effects of the direction of contribution (right M1 to left M1 vs. vice versa) and mode (parallel vs. mirror-symmetrical).

RESULTS

Phase difference

At the initiation of the parallel movement, there was a significant right-hand lead (mean \pm SD = $4.71 \pm 7.87^\circ$, $t(16) = 2.465$, $p = 0.025$, one-sample t -test), but this was not significant for mirror movement ($-0.77 \pm 4.78^\circ$, $t(16) = -0.659$, $p = 0.519$, one-sample t -test). The mode effect was significant ($t(16) = 2.447$, $p < 0.026$, paired t -test). This was consistent with previous studies (Stucchi and Viviani, 1993; Semjen et al., 1995; Treffner and Turvey, 1995, 1996; Swinnen et al., 1996; Kennerley et al., 2002; Debaere et al., 2004). By contrast, the signed phase difference averaged throughout the session showed the reverse pattern: there was a significant left-hand lead ($-16.19 \pm 18.03^\circ$, $t(16) = -3.702$, $p = 0.002$, one-sample t -test), but this was not the case for the mirror movement ($-7.959 \pm 16.988^\circ$, $t(16) = -1.932$, $p = 0.071$, one-sample t -test). The mode effect was not significant ($t(16) = -1.600$, $p = 0.129$, paired t -test). The SD around the phase difference (coordination stability) for the mirror-symmetrical mode was $21.01 \pm 12.76^\circ$, which was significantly smaller than that for the parallel mode ($36.30 \pm 21.59^\circ$; $t(16) = 4.811$, $p(16) < 0.001$; paired t -test). This indicated that the mirror-symmetrical movement was more stable than the parallel mode.

Angular velocity

During the symmetric-mirror mode, the angular velocity (mean \pm SD) of the right hand was $231.63 \pm 51.63^\circ/\text{sec}$ and that of the left hand was $222.85 \pm 52.32^\circ/\text{sec}$. During the parallel mode, the angular velocity of the right hand was $232.46 \pm$

51.81°/sec and that of the left hand was 229.03 ± 38.45°/sec. The two-way ANOVA (mode × hand) showed no significant difference in either main effects or interaction effect (mode, $F(1,16) = 0.601$, $p = 0.449$; hand, $F(1,16) = 0.405$, $p = 0.534$; interaction, $F(1,16) = 1.575$, $p = 0.228$). This finding indicated that the angular velocity was constant across the hands and modes.

During the symmetric-mirror mode, the variability of the angular velocity (mean ± SD) of the right hand was 95.26 ± 24.57°/sec and that of the left hand was 102.88 ± 25.93°/sec. During the parallel mode, the variability of the right hand was 90.90 ± 20.58°/sec and that of the left hand was 96.11 ± 25.19°/sec. The two-way repeated measures ANOVA (mode × hand) showed a significant hand effect ($F(1,16) = 5.396$; $p = 0.034$), but not a main effect of mode ($F(1,16) = 3.330$; $p = 0.087$) or an interaction effect ($F(1,16) = 0.536$; $p = 0.475$). This finding indicated that the right hand was more stable than the left hand, irrespective of the mode.

Interaction between the hands

The two-way ANOVA (contribution direction × mode) indicated a significant interaction effect ($F(1,16) = 5.021$; $p = 0.040$; Figure 3, top). *Post hoc* analysis with the Bonferroni correction indicated that the contribution from the right hand to the left hand was significantly larger than vice versa during the mirror-symmetrical mode ($t(16) = 2.791$; $p = 0.013$), but not during the parallel mode ($t(16) = 0.035$; $p = 0.972$). There was no significant main effect of contribution direction ($F(1,16) = 1.468$; $p = 0.243$) or mode ($F(1,16) = 3.757$; $p = 0.070$).

fMRI ROI analysis

The two-way ANOVA (contribution direction \times mode) of the fMRI data indicated a significant interaction effect ($F(1,16) = 5.493$; $p = 0.032$; Figure 3, bottom). *Post hoc* analysis with the Bonferroni correction indicated that the contribution from the left M1 to the right M1 was significantly larger than vice versa during the mirror-symmetrical mode ($t(16) = 2.555$; $p = 0.021$), but not during the parallel mode ($t(16) = 0.299$; $p = 0.769$). There was no significant main effect of contribution direction ($F(1,16) = 1.998$; $p = 0.177$) or mode ($F(1,16) = 2.457$; $p = 0.137$). During the rest session, the difference between the contribution from the left M1 to the right M1 and vice versa was not significant ($t(16) = 0.264$; $p = 0.795$).

There was no significant correlation between the NCR of the hands and that of the M1 activity, probably reflecting the fact that the interaction between the hands might represent the effect of both cortical cross-talk through the corpus callosum, and subcortical neural cross-talk through the ipsilateral corticospinal tract.

DISCUSSION

Kinematic analysis

Phase stability during bimanual movement

Regarding the initiation phase difference, the right hand leads the left hand, particularly during parallel movement. This is consistent with previous studies (Stucchi and Viviani, 1993; Semjen et al., 1995; Treffner and Turvey, 1995, 1996; Swinnen et al., 1996; Kennerley et al., 2002; Debaere et al., 2004). By contrast, on average during movement, the left hand leads the right hand. This tendency was particularly prominent during parallel movement. I utilized the clockwise rotation for the parallel mode in which the left (subdominant) hand led the right hand. Byblow et al. (2000) reported that the direction of the rotation had an effect on the hand that “led” in asymmetric patterns, which varied between the anti-clockwise (dominant hand) and clockwise (subdominant hand) directions. Byblow et al. (2000) suggested that neither handedness nor time-keeping localization was likely to be the cause of this phenomenon. The signed phase difference explains a relative phase between left and right, representing instantaneous causality, whereas the MAR model for two time-series provides causality from some past points to future points, and thus a better evaluation of cross-talk is expected. Actually the likelihood function using the kinematic data showed the superiority of our MAR model over the signed phase difference model (data not shown).

The SD of the phase difference between the hands was significantly smaller during mirror-symmetrical movement than during parallel movement. This finding confirms the previous studies showing that mirror-symmetrical movement is more stable than parallel movement.

Right hand dominance during mirror-symmetrical movement

The time-series analysis of the kinematic data using Akaike causality showed that the asymmetric causality from the right hand to the left hand was specific to mirror-symmetrical movement. This right-hand dominance suggests two points. First, it is consistent with the idea of cross-talk, such that the control signals directed to one hand are also sent to the other hand during mirror-symmetrical movement, which in turn stabilizes the movement. Second, the left hemisphere is dominant for this inter-manual cross-talk, because the movement of the left hand is more strongly influenced by the right-hand movement than vice versa.

Neuronal activities

Left M1 dominance during mirror-symmetrical movement

Corresponding to the kinematic results, the fMRI data revealed that the asymmetric causality from the left M1 to the right M1 was specific to mirror-symmetrical movement. This left hemisphere dominance in the cortico-cortical relationship between the bilateral M1s implies that the cross-talk or signal gating occurs at the transcallosal level during mirror-symmetrical movement.

Paired TMS studies have provided evidence that the motor cortex has clear interhemispheric facilitatory effects (Ugawa et al., 1993) and inhibitory effects (Ferber et al., 1992), probably working via the corpus callosum (Di Lazzaro et al., 1998). Whereas trans-callosal inhibition seems to play a crucial role in suppressing the mirror-symmetrical activation of the ipsilateral motor cortex during intended unilateral hand motor tasks (Nass, 1985), the functional significance of this facilitatory effect is unknown, particularly during bimanual movement. However, the

present findings and the unstable bimanual coordination in callosotomy patients raise the possibility that high-level cortico-cortical interference from the dominant hemisphere occurs in the non-dominant M1 during bimanual mirror-symmetrical movement.

Possible pathways for interhemispheric interaction

The TMS literature suggests a physiologically relevant connection among both of the M1s as documented in the intact human brain (Ferber et al., 1992; Meyer et al., 1995; Di Lazzaro et al., 1998) and the lesioned human brain (Boroojerdi et al., 1996; Murase et al., 2004; Duque et al., 2005). Using interhemispheric inhibition by means of TMS, Murase et al. (2004) showed an abnormally high interhemispheric inhibitory drive from the M1 in the intact hemisphere to the M1 in the lesioned hemisphere during the process of generation of a voluntary movement by the paretic hand. This finding suggests that motor output from the lesioned hemisphere might be additionally influenced by pathologically enhanced inhibitory influences from the intact hemisphere. This physiological evidence of a relevant connection among both M1s prompted us to examine the effective connectivity between them.

Anatomically, the direct connection between the bilateral M1s is known to be sparse in non-human primates (Rouiller et al., 1994; Liu et al., 2002). Instead, a dense indirect connection between the left and right M1s exists via the SMAs (Morecraft and Van Hoesen, 1992; Luppino et al., 1993; Rouiller et al., 1994; Wiesendanger et al., 1996; Liu et al., 2002) or the PMd (Marconi et al., 2003).

Recently, Wahl et al. (2007) examined the callosal motor fibers that connect

the primary motor cortices of the two hemispheres of the human brain. They examined the topography and somatotopy of the callosal motor fibers (CMFs) using a combined fMRI and diffusion-tensor imaging (DTI) fiber-tracking procedure. The functional connectivity between the M1s was measured by interhemispheric inhibition using paired-pulse TMS. The CMFs of the hand areas were represented in the posterior part of the body of the corpus callosum. This posterior location was interpreted to be caused by the prefrontal interhemispheric connection, which occupies the anterior half of the human corpus callosum. They also found a significant and topographically-specific positive correlation between the fractional anisotropy (FA) and interhemispheric inhibition; they interpreted this as evidence of a direct link between the microstructure and functional connectivity. Another study with DTI and paired-pulse TMS explored the fact that the FA of the projection from the PMd to the contralateral M1 was correlated with the TMS-indexed functional connectivity during action selection (Boorman et al., 2007). Thus, the pathways for interhemispheric interaction might be task-dependent.

During bimanual coordination, higher activation in the SMA and the right PMd during the parallel mode compared to the mirror-symmetrical mode is a well-replicated finding (Sadato et al., 1997; Toyokura et al., 1999; Immisch et al., 2001; Meyer-Lindenberg et al., 2002; Ullen et al., 2003; Debaere et al., 2004, Wenderoth et al., 2005, Aramaki et al., 2006a, b), which highlights the important role of the SMA and PMd in bimanual coordination. A TMS study in humans revealed that inter-hemispheric PMd-to-M1 interactions added to the M1-to-M1 interaction (Baumer et al., 2006). Bonzano et al. (2008) measured the absolute value of the timing difference between the simultaneous bimanual finger–thumb opposition

movements (inter-hand interval) made by multiple sclerosis patients with demyelinated lesions in the corpus callosum. The extent of the damage in the anterior callosal portions was positively correlated with the inter-hand interval, particularly the movement phase preceding the finger touch. This finding indicates that the anterior portion of the corpus callosum is essential for performing temporally-interdependent bimanual finger movements (Bonzano, et al., 2008). Thus, the interhemispheric interaction between the right and left M1 regions during mirror-symmetrical movement might be mediated indirectly by areas involved in higher motor functions, such as the SMA and the PMd, in addition to the possible direct interaction between the M1s.

Left-hemisphere dominance for bimanual coordination

Ziemann and Hallett (2001) proposed two different, although not mutually exclusive, models to explain the functional differences of the human cerebral hemispheres. One model assumes that asymmetrical motor performance is a consequence of intrinsic hemispheric specialization. The other proposes that both motor cortices have identical motor capabilities in controlling the contralateral hand, but that hemispheric differences occur due to asymmetric interactions between the two motor cortices.

Previous functional neuroimaging studies have shown left-lateralized activation during mirror-symmetrical movement (Jancke et al., 1998; Viviani et al., 1998), implying that the left hemisphere is specialized for controlling mirror-symmetrical bimanual movement. Aramaki et al. (2006b) found that activation in the right M1 was significantly weaker during the mirror-symmetrical

mode than during the parallel mode, a difference that was not observed in the left M1. They speculated that the non-dominant M1 entrusted a part of hand control to the dominant M1, implying a cortico-cortical interaction.

The present study showed that the cross-talk during mirror-symmetrical movement occurs at the level of the M1, possibly through the corpus callosum from the left hemisphere to the right. This cross-talk appears to stabilize mirror-symmetrical movement compared with non-symmetrical movement. This provides additional evidence of left-dominant asymmetric interhemispheric interaction during bimanual movement.

Methodological considerations for the evaluation of effective connectivity

Akaike causality (Akaike, 1968) has been applied previously to fMRI data by Yamashita et al. (2005) and by Wong and Ozaki (2007). Granger (1963, 1969) causality is another representative causality analysis based on the MAR model that has been applied in neuroscience research (for example, Bernasconi and Konig, 1999; Goebel et al., 2003). Granger causality analysis compares the residual variance of the full model to that of sub-models, and obtains a causality conclusion through the significance of the difference in variance. Akaike causality and Granger causality have two major similarities: first, they should both be applied with the assumption that they are based on an optimal model; and second, they both use information about a second-order moment (that is, variance, autocovariance, or spectrum) of the model, and therefore the second-order moment of the time-series model should be defined (using, for example, the MAR model). However, Akaike causality and Granger

causality use the variance information differently: the former is concerned with the partition of the variance in terms of noise variance within one model, while the latter is concerned with the additional partition of the variance of the data when additional regressors are introduced. An important merit of Akaike causality is that the computational load is less than that for Granger causality. Also, in the latter, it is ambiguous as to which feedback system should be chosen, leading to problems with pair-wise marginal causality or conditional causality. Akaike causality does not have this problem because it only looks at one feedback system. Therefore, to evaluate the causality across many regions in functional neuroimaging, Akaike causality has significant advantages over Granger causality in terms of the computational load and the unambiguous feedback system. One disadvantage of Akaike causality is that the noise-covariance matrix of the model must be diagonal; thus, it is not suitable for multiple time-series data with strong instantaneous causality, except when a latent variable can remove the common dynamics by means of a linear state-space model (Wong and Ozaki, 2007). With this, instantaneous causality can be included and the diagonal noise-covariance assumption is not violated.

The dynamic causal modeling (DCM) is a hypothesis-driven approach, which was specifically designed to evaluate the intrinsic and task-dependent influences that a particular brain area exerts over the activity of another area (Friston, 2003; Stephan et al., 2004; Grefkes et al., 2008). The DCM treats the brain as a deterministic system, in which external input causes changes in neural activity that, in turn, lead to changes in the fMRI signal. This is in contrast with the MAR model, which treats the brain as a dynamic network, the activities of which are driven by a stochastic effect termed

“innovation”. The DCM needs high anatomical–functional precision, and thus cannot be used as an exploratory tool. Due to the dramatic increase of the number of free parameters to be estimated, the number of ROIs is usually limited to eight or less. The DCM and MAR models are not mutually exclusive. In the future, MAR models including Akaike causality might be applied to neural parameters with the biophysical modeling adopted in the DCM (Stephan et al., 2004). The evaluation of effective connectivity by means of these sophisticated methodologies will contribute to the understanding of the mechanisms of bimanual coordination, such as hemispheric dominance under frequency stress (Kelso, 1984), in both normal and pathological conditions.

CONCLUSION

The asymmetric interhemispheric interaction from the left M1 to the right M1 during bimanual mirror-symmetrical movement might represent cortical-level cross-talk, which contributes to the stabilization of bimanual mirror-symmetrical movement.

ACKNOWLEDGMENTS

I would like to express my deep gratitude to Professor Norihiro Sadato for his generosity, valuable guidance and moral support throughout all this study. Appreciation is expressed to Dr. Kin Foon Kevin Wong for the advice and expertise. I wish also like to thank Dr. Motoaki Sugiura and Dr. Tohru Ozaki for help in preparing the manuscript. Finally, Gratitude is expressed to the members of Division of Cerebral Integration at National Institute for Physiological Sciences. They provided me a wonderful environment in which I could pursue my research unfettered.

REFERENCES

- Akaike, H., 1968. On the use of a linear model for the identification of feedback systems. *Ann. Inst. Stat. Math.* 20, 425-439.
- Akaike, H., 1977. On entropy maximization principle. In: Krishnaiah, P.R. (Ed.), *Application of Statistics*, North Holland, Amsterdam, pp. 27-42.
- Aoki, M., 1990. *State Space Modeling of Time Series*. Springer, New York.
- Åström, K.J., Kallstrom, C.G., 1973. Application of system identification techniques to the determination of ship dynamics. In: Eykhoff, P. (Ed.), *Identification and System Parameter Estimation*. North Holland, Amsterdam, pp. 415-424.
- Aramaki, Y., Honda, M., Okada, T., Sadato, N., 2006a. Neural correlates of the spontaneous phase transition during bimanual coordination. *Cereb. Cortex* 16 (9), 1338-1348.
- Aramaki, Y., Honda, M., Sadato, N., 2006b. Suppression of the non-dominant motor cortex during bimanual symmetric finger movement: a functional magnetic resonance imaging study. *Neuroscience* 141 (4), 2147-2153.
- Baumer, T., Bock, F., Koch, G., Lange, R., Rothwell, J.C., Siebner, H.R., Munchau, A., 2006. Magnetic stimulation of human premotor or motor cortex produces interhemispheric facilitation through distinct pathways. *J. Physiol.* 572, 857-868.

- Bernasconi, C., Konig, P., 1999. On the directionality of cortical interactions studied by structural analysis of electrophysiological recordings. *Biol. Cybern.* 81, 199-210.
- Bonzano, L., Tacchino, A., Roccatagliata, L., Abbruzzese, G., Mancardi, G.L., Bove, M., 2008. Callosal contributions to simultaneous bimanual finger movements. *J. Neurosci.* 28, 3227–3233.
- Boorman, E.D., O’Shea, J., Sebastian, C., Rushworth, M.F.S., Johansen-Berg, H. 2007. Individual differences in white-matter microstructure reflect variation in functional connectivity during choice. *Curr. Biol.* 17, 1426-1431.
- Borojerdi, B., Diefenbach, K., Ferbert, A. 1996. Transcallosal inhibition in cortical and subcortical cerebral vascular lesions. *J. Neurol. Sci.* 144(1-2), 160-170.
- Byblow, W.D., Carson, R.G., Goodman, D., 1994. Expression of asymmetries and anchoring in bimanual coordination. *Hum. Mov. Sci.* 13, 3-28.
- Byblow, W.D., Bysouth-Young, D., Summers, J.J., Carson, R.G., 1998. Performance asymmetries and coupling dynamics in the acquisition of multifrequency bimanual coordination. *Psychol. Res.* 61, 56-70.
- Byblow, W.D., Lewis, G.N., Stinear, J.W., Austin, N.J., Lynch, M.L., 2000. The subdominant hand increases in the efficacy of voluntary alterations in bimanual

- coordination. *Exp. Brain Res.* 131 (3), 366-374.
- Cattaert, D., Semjen, A., Summers, J.J., 1999. Simulating a neural cross-talk model for between-hand interference during bimanual circle drawing. *Biol. Cybern.* 81 (4), 343-358.
- Debaere, F., Wenderoth, N., Sunaert, S., Van Hecke, P., Swinnen, S.P., 2004. Cerebellar and premotor function in bimanual coordination: parametric neural responses to spatiotemporal complexity and cycling frequency. *Neuroimage* 21 (4), 1416-1427.
- de Oliveira, S.C., 2002. The neuronal basis of bimanual coordination: recent neurophysiological evidence and functional models. *Acta Psychol. (Amst.)* 10, 139-159.
- Di Lazzaro, V., Oliviero, A., Profice, P., Saturno, E., Pilato, F., Insola, A., Mazzone, P., Tonali, P., Rothwell, J.C., 1998. Comparison of descending volleys evoked by transcranial magnetic and electric stimulation in conscious humans. *Electroencephalogr. Clin. Neurophysiol.* 109, 397-401.
- Duque, J., Hummel, F., Celnik, P., Murase, N., Mazzocchio, R., Cohen, L. G. 2005. Transcallosal inhibition in chronic subcortical stroke. *Neuroimage* 28(4), 940-946.
- Evans, C.M., Baker, S.N., 2003. Task-dependent intermanual coupling of 8-Hz

discontinuities during slow finger movements. *Eur. J. Neurosci.* 18 (2), 453-456.

Ferbert, A., Priori, A., Rothwell, J.C., Day, B.L., Colebatch, J.G., Marsden, C.D., 1992. Interhemispheric inhibition of the human motor cortex. *J. Physiol.* 453, 525-546.

Franz, E.A., Eliassen, J.C., Ivry, R.B., Gazzaniga, M.S., 1996. Dissociation of spatial and temporal coupling in the bimanual movements of callosotomy patients. *Psychol. Sci.* 7, 306-310.

Friston, K.J., Ashburner, J., Poline, J.B., Frith, C.D., Heather, J.D., Frackowiak, R.S.J., 1995a. Spatial registration and normalization of images. *Hum. Brain Mapp.* 2, 165-189.

Friston, K.J., Holmes, A.P., Worsley, K.J., Poline J.B., Frith C.D., Frackowiak, R.S.J., 1995b. Statistical parametric maps in functional imaging: A general linear approach. *Hum. Brain Mapp.* 2, 189-210.

Friston, K.J., Harrison, L., Penny, W.D., 2003. Dynamic causal modelling. *Neuroimage* 19, 1273-1302.

Friston, K.J., Ashburner, J., Kiebel, S.J., Nichols, T.E., Penny, W.D., 2007. *Statistical Parametric Mapping: The Analysis of Functional Brain Images.* Academic Press, London.

- Garry, M.I., Franks, I.M., 2000. Reaction time differences in spatially constrained bilateral and unilateral movements. *Exp. Brain Res.* 131, 236-243.
- Goebel, R., Roebroeck, A., Kim, D.S., Formisano, E., 2003. Investigating directed cortical interactions in time-resolved fMRI data using vector autoregressive modeling and Granger causality mapping. *Magn. Reson. Imaging* 21, 1251-1261.
- Granger, C.W.J., 1963. Economic processes involving feedback. *Info. Control* 6, 28-48.
- Granger, C.W.J., 1969. Investigating causal relations by econometric models and cross-spectral methods. *Econometrica* 37, 424-438.
- Grefkes, C., Nowak, D. A., Eickhoff, S.B., Dafotakis, M., Kust, J., Karbe, H., Fink, G.R., 2008. Cortical connectivity after subcortical stroke assessed with functional magnetic resonance imaging. *Ann. Neurol.* 63, 236-246.
- Haaland, K.Y., Harrington, D.L., Knight, R.T., 2000. Neural representations of skilled movement. *Brain* 123, 2306-2313.
- Haken, H., Kelso, J.A., Bunz, H., 1985. A theoretical model of phase transitions in human hand movements. *Biol. Cybern.* 51, 347-356.
- Immisch, I., Waldvogel, D., van Gelderen, P., Hallett, M., 2001. The role of the

- medial wall and its anatomical variations for bimanual antiphase and in-phase movements. *Neuroimage* 14 (3), 674-684.
- Ivry, R.B., Hazeltine, B., 1999. Subcortical locus of temporal coupling in the bimanual movements of a callosotomy patient. *Hum. Move. Sci.* 18, 345-375.
- Jancke, L., Peters, M., Schlaug, G., Posse, S., Steinmetz, H., Muller-Gartner, H.M., 1998. Differential magnetic resonance signal change in human sensorimotor cortex to finger movements of different rate of the dominant and subdominant hand. *Brain Res. Cogn. Brain Res.* 6 (4), 279-284.
- Kagerer, F.A., Summers, J.J., Semjen, A.J., 2003. Instabilities during antiphase bimanual movements: are ipsilateral pathways involved? *Exp. Brain Res.* 151 (4), 489-500.
- Kalman, R.E., 1960. A new approach to linear filtering and prediction problems. *J. Basic Eng.* 82, 35-45.
- Kelso, J.A., 1984. Phase transitions and critical behavior in human bimanual coordination. *Am. J. Physiol.* 246, R1000-R1004.
- Kennerley, S.W., Diedrichsen, J., Hazeltine, E., Semjen, A., Ivry, R.B., 2002. Callosotomy patients exhibit temporal uncoupling during continuous bimanual movements. *Nat. Neurosci.* 5, 376-381.

Kitagawa, G., Gersch, W., 1996. Smoothness Priors Analysis of Time Series. Springer, New York.

Liu, J., Morel, A., Wannier, T., Rouiller, E.M., 2002. Origins of callosal projections to the supplementary motor area (SMA): a direct comparison between pre-SMA and SMA-proper in macaque monkeys. *J. Comp. Neurol.* 443 (1), 71-85.

Luppino, G., Matelli, M., Camarda, R., Rizzolatti, G., 1993. Corticocortical connections of area F3 (SMA-proper) and area F6 (pre-SMA) in the macaque monkey. *J. Comp. Neurol.* 338 (1), 114-140.

Marconi, B., Genovesio, A., Giannetti, S., Molinari, M., Caminiti, R., 2003. Callosal connections of dorso-lateral premotor cortex. *Eur. J. Neurosci.* 18 (4), 775-788.

Marteniuk, R.G., MacKenzie, C.L., 1980. Information processing in movement organization and execution. In: Nickerson, R. (Ed.) *Attention and Performance VIII*. Hillsdale, Erlbaum, pp. 29-57.

Meyer, B.U., Roricht, S., Graf von Einsiedel, H., Kruggel, F., Weindl, A. 1995. Inhibitory and excitatory interhemispheric transfers between motor cortical areas in normal humans and patients with abnormalities of the corpus callosum. *Brain* 118 (Pt 2), 429-440.

Meyer-Lindenberg, A., Ziemann, U., Hajak, G., Cohen, L., Berman, K.F., 2002.

Transitions between dynamical states of differing stability in the human brain.
Proc. Natl. Acad. Sci. USA 99 (17), 10948-10953.

Morecraft, R.J., Van Hoesen, G.W., 1992. Cingulate input to the primary and supplementary motor cortices in the rhesus monkey: evidence for somatotopy in areas 24c and 23c. *J. Comp. Neurol.* 322 (4), 471-489.

Murase, N., Duque, J., Mazzocchio, R., Cohen, LG. 2004. Influence of interhemispheric interactions on motor function in chronic stroke. *Ann Neurol* 55(3), 400-409.

Nass, R., 1985. Mirror movement asymmetries in congenital hemiparesis: the inhibition hypothesis revisited. *Neurology* 35, 1059-1062.

Oldfield, R.C., 1971. The assessment and analysis of handedness: the Edinburgh inventory. *Neuropsychologia* 9, 97-113.

Preilowski, B.F., 1972. Possible contribution of the anterior forebrain commissures to bilateral motor coordination. *Neuropsychologia* 10, 267-277.

Rogers, M.A., Bradshaw, J.L., Cunnington, R.C., Phillips, J.G., 1998. Inter-limb coupling in coordinated bimanual movement: attention and asymmetries. *Laterality* 3, 53-75.

- Rouiller, E.M., Babalian, A., Kazennikov, O., Moret, V., Yu, X.H., Wiesendanger, M., 1994. Transcallosal connections of the distal forelimb representations of the primary and supplementary motor cortical areas in macaque monkeys. *Exp. Brain Res.* 102 (2), 227-243.
- Sadato, N., Yonekura, Y., Waki, A., Yamada, H., Ishii, Y., 1997. Role of the supplementary motor area and the right premotor cortex in the coordination of bimanual finger movements. *J. Neurosci.* 17 (24), 9667-9674.
- Schöner, G., Kelso, J.A., 1988. Dynamic pattern generation in behavioral and neural systems. *Science* 239, 1513-1520.
- Semjen, A., Summers, J.J., Cattaert, D., 1995. Hand coordination in bimanual circle drawing. *J. Exp. Psychol. Hum. Percept. Perform.* 21, 1139-1157.
- Serrien, D.J., Cassidy, M.J., Brown, P., 2003. The importance of the dominant hemisphere in the organization of bimanual movements. *Hum. Brain Mapp.* 18 (4), 296-305.
- Sherwood, D.E., 1994. Hand preference, practice order, and spatial assimilations in rapid bimanual movement. *J. Mot. Behav.* 26, 123-134.
- Sirigu, A., Duhamel, J.R., Cohen, L., Pillon, B., Dubois, B., Agid, Y., 1996. The mental representation of hand movements after parietal cortex damage. *Science*

273, 1564-1568.

Spencer, R.M., Zelaznik, H.N., Diedrichsen, J., Ivry, R.B., 2003. Disrupted timing of discontinuous but not continuous movements by cerebellar lesions. *Science* 300 (5624), 1437-1439.

Stephan, K.M., Harrison, L.M., Penny, W.D., Friston, K.J., 2004. Biophysical models of fMRI responses. *Curr. Opin. Neurobiol.* 14, 629-635.

Stucchi, N., Viviani, P., 1993. Cerebral dominance and asynchrony between bimanual two-dimensional movements. *J. Exp. Psychol. Hum. Percept. Perform.* 19, 1200-1220.

Swinnen, S.P., Jardin, K., Meulenbroek, R., 1996. Between-limb asynchronies during bimanual coordination: effects of manual dominance and attentional cueing. *Neuropsychologia* 34 (12), 1203-1213.

Swinnen, S.P., Jardin, K., Meulenbroek, R., Dounskaia, N., Hofkens-van den Brandt, M., 1997. Egocentric and allocentric constraints in the expression of patterns of interlimb coordination. *J. Cogn. Neurosci.* 9, 348-377.

Toyokura, M., Muro, I., Komiya, T., Obara, M., 1999. Relation of bimanual coordination to activation in the sensorimotor cortex and supplementary motor area: analysis using functional magnetic resonance imaging. *Brain Res. Bull.* 48

(2), 211-217.

Treffner, P., Turvey, M., 1995. Handedness and the asymmetric dynamics of bimanual rhythmic coordination. *J. Exp. Psychol. Hum. Percept. Perform.* 21, 318-333.

Treffner, P.J., Turvey, M.T., 1996. Symmetry, broken symmetry, and handedness in bimanual coordination dynamics. *Exp. Brain Res.* 107, 463-478.

Ugawa, Y., Hanajima, R., Kanazawa, I., 1993. Interhemispheric facilitation of the hand area of the human motor cortex. *Neurosci. Lett.* 160 (2), 153-155.

Ullen, F., Forssberg, H., Ehrsson, H., 2003. Neural networks for the coordination of the hands in time. *J. Neurophysiol.* 89 (2), 1126-1135.

Viviani, P.D., Perani, D., Grassi, F., Bettinardi, V., Fazio, F., 1998. Hemispheric asymmetries and bimanual asynchrony in left- and right-handers. *Exp. Brain Res.* 120 (4), 531-536.

Wahl, M., Lauterbach-Soon, B., Hattingen, E., Jung, P., Singer, O., Volz, S., Klein, J.C., Steinmetz, H., Ziemann, U., 2007. Human motor corpus callosum: topography, somatotopy, and link between microstructure and function. *J. Neurosci.* 27(45), 12132-12138.

Walter, C.B., Swinnen, S.P., 1992. Adaptive tuning of interlimb attraction to

facilitate bimanual decoupling. *J. Mot. Behav.* 24 (1), 95-104.

Wenderoth, N., Debaere, F., Sunaert, S., Swinnen, S.P., 2005. Spatial interference during bimanual coordination: differential brain networks associated with control of movement amplitude and direction. *Hum. Brain Mapp.* 26 (4), 286-300.

Wiesendanger, M., Rouiller, E.M., Kazennikov, O., Perrig, S., 1996. Is the supplementary motor area a bilaterally organized system? *Adv. Neurol.* 70, 85-93.

Wong, K.F.K., Ozaki, T., 2007. Akaike causality in state space: Instantaneous causality between visual cortex in fMRI time series. *Biol. Cybern.* 97 (2), 151-157.

Yamashita, O., Sadato, N., Okada, T., Ozaki, T., 2005. Evaluating frequency-wise directed connectivity of BOLD signals applying relative power contribution with the linear multivariate time-series models. *Neuroimage* 25 (2), 478-490.

Yousry, T.A., Schmid, U.D., Alkadhi, H., Schmidt, D., Peraud, A., Buettner, A., Winkler, P., 1997. Localization of the motor hand area to a knob on the precentral gyrus. a new landmark. *Brain* 120 (1), 141-157.

Ziemann, U., Hallett, M., 2001. Hemispheric asymmetry of ipsilateral motor cortex activation during unimanual motor tasks: further evidence for motor dominance. *Clin. Neurophysiol.* 112, 107-113.

TABLE**Table 1**

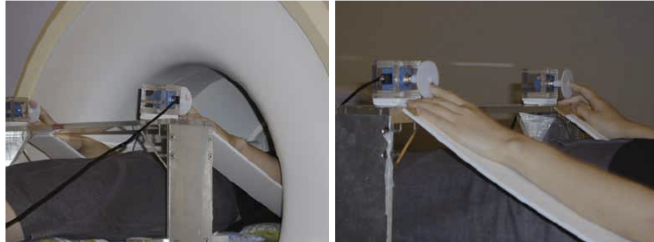
Normalized coordinates of the M1s of subjects

subject	left M1				right M1			
	MNI coordinates			<i>T</i> value	MNI coordinates			<i>T</i> value
	x	y	z		x	y	z	
1	-44	-22	54	10.79	32	-24	54	10.09
2	-34	-28	58	17.61	36	-28	60	25.16
3	-38	-26	60	32.13	30	-32	62	22.21
4	-40	-20	64	20.83	36	-14	64	19.89
5	-30	-26	50	22.26	40	-24	52	27.94
6	-38	-28	60	21.77	32	-32	56	22.08
7	-36	-26	56	15.48	46	-30	54	20.31
8	-38	-24	56	15.58	38	-26	60	30.13
9	-34	-24	56	13.01	36	-22	58	19.20
10	-42	-16	62	24.13	38	-28	60	14.08
11	-44	-18	56	24.11	44	-20	52	12.89
12	-42	-22	58	29.47	42	-24	62	31.19
13	-38	-24	62	21.48	32	-28	58	16.58
14	-36	-26	60	17.93	42	-14	54	23.31
15	-42	-20	52	13.43	36	-22	54	16.97
16	-36	-18	60	23.47	32	-26	64	24.32
17	-42	-20	52	11.01	44	-14	52	16.15
mean	-38.47	-22.82	57.41	19.68	37.41	-24.00	57.41	20.74
S.D.	3.91	3.68	3.92	6.12	4.94	5.83	4.23	5.96

MNI coordinates (x, y, z) and *T* value of the M1s of participants. The functionally and anatomically defined M1s of each subject were normalized into space registered by MNI coordinates.

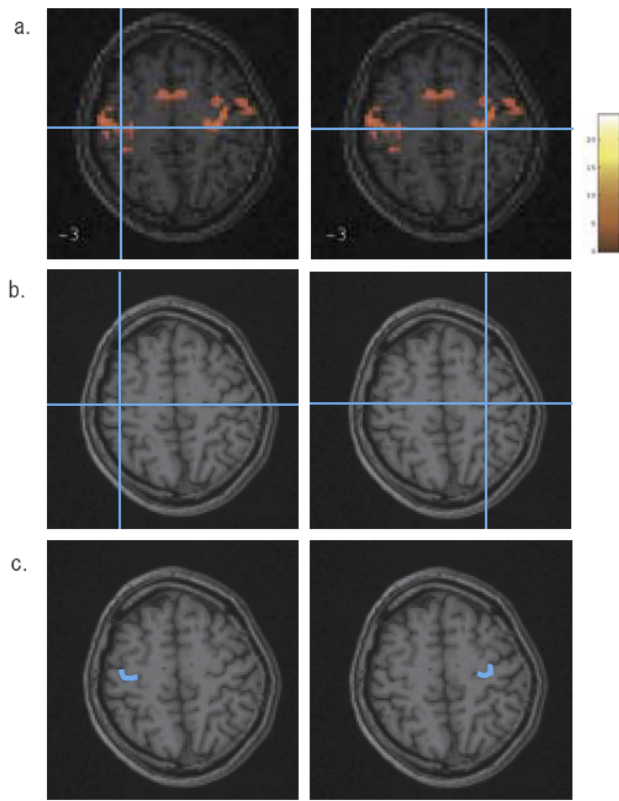
FIGURES and FIGURE LEGENDS

Figure 1.



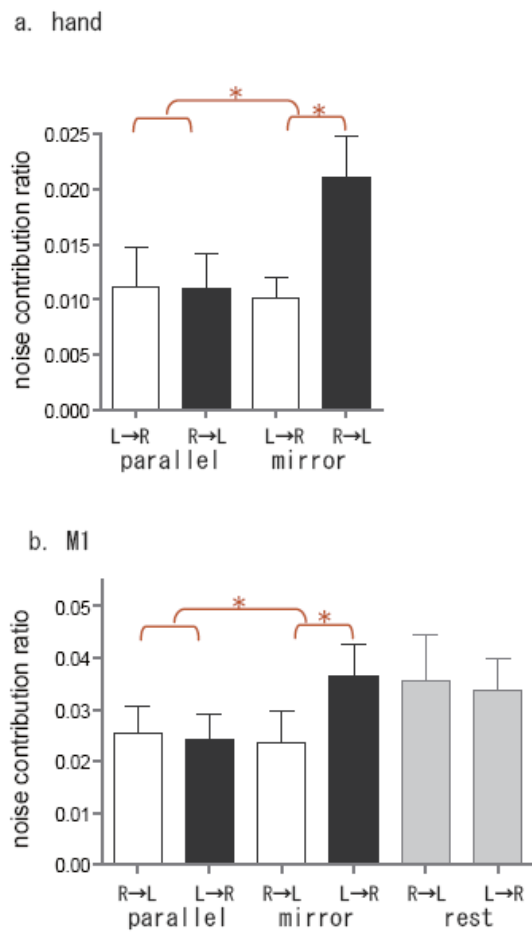
Experimental setup. Subjects lay supine in the scanner with their elbows and wrist junctions placed on the nonferromagnetic frame in a slightly flexed and pronated position. During scanning, each participant's head was located at the center of the magnet, while both their hands and the discs were outside of the magnet. In this position, the subjects could not see their hand movements (left). The discs were rotated with the index fingers (right). Hand movements were registered automatically with the input devices connected to a personal computer.

Figure 2.



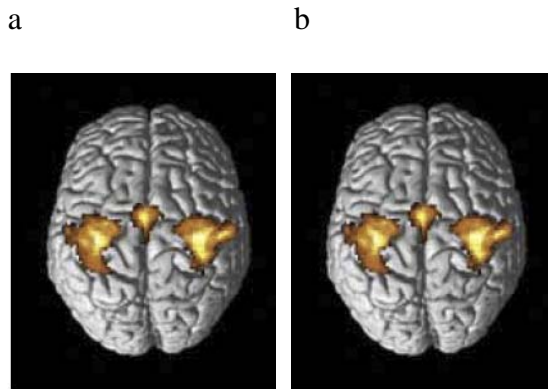
ROIs of the M1s. The ROIs were defined as the local maxima of the activated areas by the bimanual rotation of the discs (a), within or closest to the hand knob structure of the inverted-omega shape (b) that was a landmark of the hand area (c, blue blobs). (a) SPMs of the enhanced neural activity during bimanual movement. Activated foci are superimposed on the transaxial plane of the T1-weighted high-resolution MRIs of the subjects. The T score is as indicated by the color bar; the statistical significance increases as red changes to white. The threshold for the $SPM\{t\}$ was set at a family-wise error rate (FWE) of $p < 0.001$. The cross-hair indicates the ROIs.

Figure 3.



(a) NCR between hands during the parallel mode and the mirror mode. The contribution from the left hand to the right hand is shown by open bars, and the contribution from the right hand to the left hand is shown by closed bars. (b) NCR between M1s during parallel, mirror, and rest modes. The contribution from the left M1 to the right M1 is shown by open bars, and the contribution from the right M1 to the left M1 is shown by closed bars during the mirror and parallel modes. During the rest mode, the NCRs of both directions are shown by closed gray bars. $*p < 0.05$ (two-way ANOVA).

Figure 4.



Statistical parametric map of the average neural activity within the group during parallel (a) and mirror (b) movement. The activities while performing the task were superimposed on surface rendered high-resolution MRIs unrelated to the subjects of the present study. The threshold for the $SPM\{t\}$ was set at a family-wise error rate (FWE) of $p < 0.001$. The prominent foci were bilateral M1s, bilateral dorsal premotor areas and supplementary motor areas in both modes. As to the intensity of the activation, contrary to the effective connectivity, there was no significant difference between the two modes.

$$G = \begin{bmatrix} 1 & 0 & 0 \\ 0 & \dots & 0 \\ \vdots & & \vdots \\ 0 & \dots & 0 \\ 0 & 1 & 0 \\ 0 & 0 & 1 \end{bmatrix}$$

$$H_j = \begin{bmatrix} h(j) & 0 & \dots & 0 & 1 & 0 \\ 0 & 1 & 0 & 0 & 0 & \dots & 0 & 0 & 1 \end{bmatrix}$$

$$h(j) = \begin{cases} (1\ 0\ 0\ 0) & \text{if } j=1 \\ (0\ 1\ 0\ 0) & \text{if } j=2 \\ (0\ 0\ 1\ 0) & \text{if } j=3 \\ (0\ 0\ 0\ 1) & \text{if } j=4 \end{cases}$$

$$Q = \begin{bmatrix} \sigma^{(1)2} & 0 & 0 \\ 0 & \sigma^{(2)2} & 0 \\ 0 & 0 & \sigma^{(3)2} \end{bmatrix}$$

$$R=0$$

Here, F was a $(p+2) \times (p+2)$ square matrix, a transitional matrix of state x_t from state x_{t-1} . It can be considered as a block diagonal matrix of a $p \times p$ matrix and a 2×2 matrix. The $p \times p$ block matrix was intended to explain the common dynamics, and the 2×2 block was intended to explain a coupling of the remaining information. p therefore denoted the AR order of the process of the common dynamics. ω_t was a three-dimensional system noise vector. With this given G , the three elements of ω_t were distributed to the first, the second to last, and the last element of x_t .

H was a $2 \times (p+2)$ observation matrix. When we fitted this model, we allowed at each time step H choosing from H_1, H_2, H_3 , or H_4 , whichever maximized the likelihood function at that time step. The four different H values gave a degree of

freedom to the jittering motion of the rotating fingers. In the case of (1 0 0 0), the right hand phase preceded the left hand phase by one time point (10 msec). In the case of (0 1 0 0), the precedence of the phases of both hands was the same. In the case of (0 0 1 0), the left hand preceded the right hand by one time point (10 msec). In the case of (0 0 0 1), the precedence of the left hand was two time points (20 msec). We adapted this procedure such that the fitted model explained the data by absorbing the fluctuation of the unsteady hand movement.

Q was the variance of ω_t and R was the variance of observation error ε_t . Q was assumed to be the diagonal of three elements: $\sigma^{(1)2}$, $\sigma^{(2)2}$, and $\sigma^{(3)2}$. For simplicity, R was set to zero, as the measurement error was less than 1° .

The set of free parameters comprised $p+4$ parameters in F and three parameters in Q . For each value of p , a set of model parameters was estimated from the given data by the maximum likelihood method. Given a set of model parameters, the computation of the likelihood from the errors of the data predictions, as obtained by the application of the Kalman filter, was straightforward (see Åström and Kallstrom, 1973, for a detailed treatment). Comprehensive introductions to state space models and Kalman filtering have been provided by Kalman (1960) and by Kitagawa and Gersch (1996).

As p increased, the likelihood function also increased; however, an optimal order p was chosen using the Akaike Information Criterion (AIC), such that the model with the smallest AIC was selected (Akaike, 1977).

Appendix B

State space modeling of preprocessed fMRI data

State space modeling was used to analyze the preprocessed fMRI time series. The idea of a hidden variable was applied again with a modification of the parameterization. For the fMRI data, we restricted the common dynamics to the first order, and let the coupling part have a higher order; by contrast, for the kinematic data, we allowed the common dynamics to have a higher order but allowed the coupling part only the first order, because the fMRI data did not show any prominent common periodicity as the kinematic data did. The state space model described in Appendix A was applied, with the following parameterization:

$$F = \begin{pmatrix} f_{111} & f_{112} & 1 & 0 & & & & & 1 \\ f_{121} & f_{122} & 0 & 1 & & & & & c \\ f_{211} & f_{212} & & & 1 & 0 & & & 0 \\ f_{221} & f_{222} & & & 0 & 1 & & & \\ \vdots & & & & & & \ddots & & \vdots \\ f_{p11} & f_{p12} & \dots & & & & 0 & 0 & \\ f_{p21} & f_{p22} & & & & & 0 & 0 & 0 \\ 0 & 0 & & & \dots & & 0 & 0.05 & \end{pmatrix}$$

(p : AR order)

$$G = \begin{bmatrix} 1 & 0 & 0 \\ 0 & 1 & 0 \\ 0 & \dots & 0 \\ \vdots & & \vdots \\ 0 & \dots & 0 \\ 0 & 0 & 1 \end{bmatrix}$$

$$H_j = \begin{bmatrix} 1 & 0 & 0 & 0 & 0 & \dots & 0 \\ 0 & 1 & 0 & 0 & 0 & \dots & 0 \end{bmatrix}$$

$$Q = \begin{bmatrix} \sigma^{(1)2} & 0 & 0 \\ 0 & \sigma^{(2)2} & 0 \\ 0 & 0 & \sigma^{(3)2} \end{bmatrix}$$

$$R = \begin{bmatrix} 0.042 & 0 \\ 0 & 0.042 \end{bmatrix}$$

Here, F was a $(2p+1) \times (2p+1)$ square matrix. The upper left $2p \times 2p$ element was a canonical form of a bivariate AR(p) process (Aoki, 1990), capturing the main characteristics of the time series. p was chosen using the AIC, such that the bivariate MAR model with the smallest AIC was selected (Akaike, 1977). The common dynamics process, aimed at capturing the instantaneous dynamics, was adopted by introducing the last element of F . This near-white AR process was coupled to the observed states by the coefficients 1 and c (Wong and Ozaki, 2007).

The three elements of the system noise ω_t were distributed to the first, the second, and the last element of x_t through the designed G . As the coupling of the hidden variable and the observed states happened in F , the observation matrix H helped in taking only the first two elements of x_t .

Again, Q was the variance of ω_t and R was the variance of the observation error ε_t . Q was assumed to be the diagonal of three elements: $\sigma^{(1)2}$, $\sigma^{(2)2}$, and $\sigma^{(3)2}$. As the measurement error of the fMRI data was about ± 0.25 , we set the observation noise variance at 0.042.

The set of free parameters included $4p+1$ parameters in F and three parameters in Q . These were again estimated by the maximum likelihood method.